ELK1-mediated upregulation of lncRNA LBX2-AS1 facilitates cell proliferation and invasion via regulating miR-491-5p/S100A11 axis in colorectal cancer

GANG MA[1], WEIJIE DAI[1], JUAN ZHANG[1], QIANJUN LI[1], BIAO GU[2], YAQI SONG[3] and XIAOZHONG YANG[1]

[1]Division of Gastroenterology, Departments of [2]Thoracic Surgery and [3]Radiation Oncology,
The Affiliated Huai'an No. 1 People's Hospital of Nanjing Medical University, Huai'an, Jiangsu 223300, P.R. China

Received August 13, 2020; Accepted April 29, 2021

DOI: 10.3892/ijmm.2021.4971

Abstract. The aim of the present study was to investigate the role and regulatory mechanism of LBX2 antisense RNA 1 (LBX2-AS1) in colorectal cancer. Firstly, LBX2-AS1 expression was detected using reverse transcription-quantitative PCR in colorectal cancer tissues and cells, and its prognostic and diagnostic efficacy was assessed in a colorectal cancer cohort (n=145). Subcellular fractionation assay of LBX2-AS1 was performed. Secondly, the effects of LBX2-AS1 and microRNA (miR)-491-5p on colorectal cancer cell proliferation, apoptosis, migration and invasion were investigated by a series of functional assays. Thirdly, RNA immunoprecipitation, dual-luciferase reporter and gain and loss of function assays were carried out to analyze the interactions between ETS transcription factor ELK1 (ELK1) and LBX2-AS1, as well as LBX2-AS1, miR-491-5p and S100A11. The results showed that LBX2-AS1 was upregulated both in colorectal cancer tissues and cells, which was distributed in the cytoplasm and nucleus of colorectal cancer cells. Clinically, high LBX2-AS1 expression could be an independent prognostic factor for colorectal cancer. Furthermore, relative operating characteristic curve analysis showed that LBX2-AS1 was a sensitive diagnostic marker for colorectal cancer. Highly expressed ELK1, as a transcription factor, could bind to the two conserved sites in the promoter region of LBX2-AS1, thereby activating the transcription of LBX2-AS1. Silencing LBX2-AS1 markedly inhibited proliferative, migratory and invasive abilities of colorectal cancer cells. miR-491-5p expression was downregulated, while S100A11 expression was upregulated in colorectal cancer tissues and cells. Dual-luciferase reporter assays confirmed that LBX2-AS1 could block S100A11 degradation via competitively binding to miR-491-5p. Furthermore, LBX2-AS1 overexpression could notably reverse the inhibitory effect of miR-491-5p on proliferation and invasion of colorectal cancer cells. Taken together, LBX2-AS1 induced by transcription factor ELK1 may facilitate colorectal cancer cell proliferation and invasion via regulation of the miR-491-5p/S100A11 axis. Thus, LBX2-AS1 could be an underlying prognostic and diagnostic marker for colorectal cancer.

Correspondence to: Professor Xiaozhong Yang, Division of Gastroenterology, The Affiliated Huai'an No. 1 People's Hospital of Nanjing Medical University, 1 Huanghe West Road, Huaiyin, Huai'an, Jiangsu 223300, P.R. China
E-mail: yangxz1023@126.com

Abbreviations: ncRNA, non-coding RNA; lncRNA, long non-coding RNA; miRNAs, microRNAs; RT-qPCR, reverse transcription-quantitative PCR; RIP, RNA immunoprecipitation; CCK-8, Cell Counting Kit-8; EMT, epithelial-mesenchymal transition; OS, overall survival; DFS, disease-free survival

Key words: colorectal cancer, LBX2 antisense RNA 1, ETS transcription factor ELK1, proliferation, invasion, miR-491-5p, S100A11

Introduction

Colorectal cancer is one of the most frequently diagnosed malignancies, characterized by unfavorable morbidity and mortality rates (1). Despite advancements in treatment strategies, including surgical resection, chemotherapy, radiotherapy, targeted therapy and immunotherapy, the overall survival (OS) time of patients with colorectal cancer has not been markedly prolonged (2-4). Postoperative recurrence and metastasis of colorectal cancer have been considered as the main causes of death (5). Thus, there is an urgent requirement to actively search for reliable molecules involved in the pathogenesis of colorectal cancer.

It has been widely accepted that long-term effects of environmental factors and genetic inheritance could contribute to colorectal cancer progression (6). Extensive research findings have shown that the multi-level regulation of protein coding genes by non-coding RNA (ncRNA) may be associated with colorectal cancer progression (7-9). The Encyclopedia of DNA elements project launched in 2003 has found that nearly 65% of genes are transcribed into ncRNAs (7-9). Long ncRNA (lncRNA; >200 bp), a class of ncRNAs, accounts for >80% of all ncRNAs (7-9). LncRNAs have a variety of biological functions and are widely involved in various cellular activities (10). It has been confirmed that LBX2 antisense RNA1

(LBX2-AS1), which is located on 2p13.1, may drive the progression of several cancers, including esophageal squamous cell carcinoma (11), lung carcinoma (12), gastric carcinoma (13) and liver cancer (14), by binding with various microRNAs (miRNAs/miRs) such as miR-219a-2-3p, miR-4685-5p, miR-491-5p and miR-4766-5p. Nonetheless, the role and regulatory mechanisms of LBX2-AS1 in colorectal cancer remain to be elucidated.

Recent studies have shown that a number of transcription factors are abnormally expressed in tumors and participate in the induction of lncRNA expression (15-17). Furthermore, lncRNA can serve as competing endogenous RNAs to block the effect of miRNA on mRNA, thereby indirectly enhancing the stability of mRNA and increasing the expression of mRNA (18-20). The present study aimed to investigate the role and regulatory mechanism of LBX2-AS1 in colorectal cancer.

Materials and methods

Tissue specimens. Overall, 145 colorectal cancer tissues and corresponding adjacent normal tissues were gathered from the Affiliated Huai'an No. 1 People's Hospital of Nanjing Medical University (Huai'an, China) between January 2014 and July 2015. None of the patients had been treated with chemotherapy or radiotherapy prior to operation. All specimens were confirmed by at least two pathologists as colorectal cancer. Normal colorectal mucosa epithelium tissues >5 cm from the edge of the tumor were obtained as adjacent normal controls. Complete clinical information was collected and all patients were followed up for >60 months. Among them, 10 cases of colorectal cancer tissue specimens and corresponding adjacent normal tissues were used for microarray analysis (Shanghai OE Biotech Co., Ltd.). Differentially expressed genes were visualized into a heatmap via the R language package (version 3.4.1) (21). This study strictly followed the Declaration of Helsinki and acquired the approval of the ethics committee of the Affiliated Huai'an No. 1 People's Hospital of Nanjing Medical University (approval no. 2014059). All participants provided signed informed consent.

Bioinformatics analysis. LBX2-AS1, ETS transcription factor ELK1 (ELK1) and S100A11 expression levels were evaluated in colorectal cancer tissues and normal tissues in The Cancer Genome Atlas (TCGA)/The Genotype-Tissue Expression (GTEx) database using the GEPIA tool (http://gepia2.cancer-pku.cn/) (22). Using this tool, the differences in LBX2-AS1 or S100A11 expression among different stages (TNM stages I-III and IV) were also assessed in colorectal cancer samples (22). Overall and disease-free survival analyses were performed between high and low LBX2-AS1 expression groups using the GEPIA tool (22). Transcription factors that could bind to the promoter of LBX2-AS1 were predicted through comprehensive analysis of the JASPAR (http://jaspar.genereg.net) (23) and PROMO (http://alggen.lsi.upc.es/cgi-bin/promo_v3/promo/promoinit.cgi?dirDB=TF_8.3) databases (24). Subcellular locations of LBX2-AS1 were predicted via the lncATLAS (http://lncatlas.crg.eu/) (25) and lncLocator (http://www.csbio.sjtu.edu.cn/bioinf/lncLocator/) databases (26). The starBase version 3.0 (http://starbase.sysu.edu.cn/) database (27) was employed to predict target miRNAs of LBX2-AS1. The correlation between hsa-miR-491-5p and LBX2-AS1 expression was determined using Pearson's correlation in the starBase database. Differentially expressed genes (DEGs) with |log2fold-change|>1 and P<0.05 were analyzed between colorectal cancer and normal tissues in TCGA database, which were visualized into heatmap and volcano plots using the R language package (version 3.4.1) (21). From the UALCAN database (http://ualcan.path.uab.edu/), S100A11 expression was detected in colorectal cancer and normal tissues using data from the Clinical Proteomic Tumor Analysis Consortium (CPTAC) dataset (28). Furthermore, S100A11 expression was determined in a pan-cancer analysis using the GEPIA tool (22).

Cell culture. Human normal colorectal mucosa FHC cell line, three colon cancer cell lines (including LoVo, SW620 and HCT116) and one colorectal cancer cell line HT29 that were authenticated by STR profiling were acquired from American Type Culture Collection (ATCC). Cells were grown in RPMI-1640 medium (HyClone; Cytiva) with 10% FBS (HyClone; Cytiva), 100 U/ml penicillin and 100 μg/ml streptomycin at 37˚C and 5% CO_2 in a humidified incubator.

Reverse transcription-quantitative PCR (RT-qPCR). RNA extraction from cells or tissues was carried out using TRIzol® reagent (Invitrogen; Thermo Fisher Scientific, Inc.). RNA concentration and OD value of 2 μl RNA solution were determined using a NanoDrop™ 2000 ultra-micro spectrophotometer (NanoDrop Technologies; Thermo Fisher Scientific, Inc.). Reverse transcription was performed using PrimeScript RT Reagent kit (Takara Biotechnology Co., Ltd.) at 37˚C for 45 min and at 85˚C for 5 min. GAPDH was regarded as an internal reference. qPCR was performed using SYBR Premix EX Taq II (Takara Bio, Inc.) and the ABI 7900 fluorescence quantitative PCR instrument (Applied Biosystems; Thermo Fisher Scientific, Inc.). The thermocycling conditions were as follows: 94˚C for 2 min; 40 cycles of 94˚C for 15 sec and 60˚C for 45 sec. Primer sequences are listed in Table I. The expression levels of LBX2-AS1, ELK1 and S100A11 were normalized to GAPDH, while miR-491-5p expression was normalized to U6. Relative expression levels were determined using the $2^{-\Delta\Delta Cq}$ method (29).

Transfection. SW620 and HT29 cells ($3.0x10^5$) were incubated in a 6-well plate for 24 h. Then, 2 μg small interfering RNAs (siRNAs) targeting ELK1 (5'-AACCACCCGCCACTCTTCCT-3'; Shanghai GenePharma Co., Ltd.) and LBX2-AS1 (5'-CCAUUAAUUCAGCAAACAUUCCUTT-3'; Shanghai GenePharma Co., Ltd.) and corresponding scramble siRNA controls (5'-UUCUCCGAACGUGUCACGUTT-3'; Shanghai GenePharma Co., Ltd.) were separately transfected into each well via PowerFect™ In Vitro siRNA Transfection Reagent (SignaGen Laboratories). A total of 2 μg pcDNA3.1-ELK1, pcDNA3.1-LBX2-AS1 plasmids and corresponding empty vectors (Shanghai GenePharma Co., Ltd.), which were used as controls, were added to each well via Lipofectamine® 2000 (Invitrogen; Thermo Fisher Scientific, Inc.). Furthermore, 50 nM miR-491-5p mimics (5'-AGUGGGGAACCCUUCCAUGAGG-3'; Shanghai GenePharma Co., Ltd.) and mimic negative controls (NCs; 5'-CAGCUGGUUGAAGGGGACCAAA-3';

Table I. Primer sequences for reverse transcription-quantitative PCR.

Genes	Primer sequences (5'→3')
LBX2-AS1	F: ATAGCTCATGTCCTGTCCTTC
	R: ACTTCCTTGTTGCCGATATC
ELK1	F: TTGTGTCCTACCCAGAGGTTG
	R: GCTATGGCCGAGGTTACAGA
miR-491-5p	F: GGAGTGGGGAACCCTTCC
	R: GTGCAGGGTCCGAGGT
S100A11	F: GCGGGAAGGATGGAAACAACA
	R: TCATCATGCGGTCAAGGACAC
GAPDH	F: GGAGCGAGATCCCTCCAAAAT
	R: GGCTGTTGTCATACTTCTCATGG
U6	F: GGCAGATCAATGTTTCCACAGA
	R: CAGTACCGACAACTGAGAGGA

F, forward; R, reverse; LBX2-AS1, LBX2 antisense RNA 1; miR, microRNA; ELK1, ETS transcription factor ELK1.

Shanghai GenePharma Co., Ltd.) were transfected into cells. After transfection for 48 h at room temperature, RT-qPCR was performed to validate transfection efficacy.

RNA immunoprecipitation (RIP) assay. RIP was performed using RNA Binding Protein Immunoprecipitation kit (EMD Millipore). SW620 and HT29 cells were lysed using RIP lysis buffer (Beyotime Institute of Biotechnology). The lysate was centrifuged at 12,000 x g for 30 min at 4˚C, and the supernatant was incubated with magnetic beads coated with anti-IgG antibody (cat. no. ab109489; Abcam) overnight at 4˚C, followed by digestion with proteinase K buffer. The beads were washed three times with the washing buffer (50 mM Tris-HCl, 300 mM NaCl pH 7.4, 1 mM $MgCl_2$, 0.1% NP-40). The immunoprecipitation RNA was extracted using TRIzol® (Beyotime Institute of Biotechnology) and analyzed via RT-qPCR.

Dual-luciferase reporter assay. Luciferase reporter vector (Shanghai GenePharma Co., Ltd.) with the LBX2-AS1 promoter -2,500 kb ~ +245 bp full sequence and LBX2-AS1 promoter deletion plasmids were transfected into 293T cells (ATCC) using Lipofectamine® 2000 (Invitrogen; Thermo Fisher Scientific, Inc.). The fluorescence signal was monitored after 24 h of transfection. LBX2-AS1 wild-type (LBX2-AS1-wt) and mutant (LBX2-AS1-mut), S100A11 wild-type (S100A11-wt) and mutant (S100A11-mut) sequences were inserted into the pmirGLO vector (Promega Corporation). Mutant sequences were generated using a Hieff Mut™ Site-Directed Mutagenesis kit (cat. no. 11003ES10; Shanghai Yeasen Biotechnology Co., Ltd.). miR-491-5p mimics/controls were co-transfected with LBX2-AS1-wt/LBX2-AS1-mut or S100A11-wt/S100A11-mut using Lipofectamine 2000. After 48 h, the cells were collected and luciferase activity was determined using a Dual-Luciferase Reporter Assay System (Beyotime Institute of Biotechnology). These results were standardized in line with *Renilla* luciferase activity.

Cell counting kit-8 (CCK-8) assay. SW620 and HT29 cells ($2.5x10^4$) were seeded into a 96-well plate for 2-3 h. Then, 10 μl CCK-8 reagent (Beyotime Institute of Biotechnology) was added to the corresponding wells. Cells were taken out 24, 48, 72 and 96 h after inoculation, and the absorbance was tested at 450 nm utilizing an automatic microplate reader (Bio-Rad Laboratories, Inc.).

Clone formation assay. SW620 and HT29 cells were seeded into a 6-well plate (3,000 cells/well). Then, 2.5 ml complete medium (HyClone; Cytiva) was added to each well and cells were cultured for 10-14 days. After discarding the supernatant, the cells were fixed with 4% paraformaldehyde at room temperature for 15 min and stained with 2% crystal violet staining solution at room temperature for 10 min. Finally, the colony number was counted. A colony was defined as consisting of at least 50 cells.

Flow cytometry assay. SW620 and HT29 cell apoptosis assay was carried out using an Annexin V-APC/PI apoptosis detection kit (Nanjing KeyGen Biotech Co., Ltd.) in the dark, according to the manufacturer's instructions. Early and late apoptotic cells were detected using a BD Accuri™ C6 Plus Flow Cytometer (BD Biosciences) at an excitation wavelength of 488 nm. The results were analyzed using FlowJo software (version 10.6.2; FlowJo LLC).

ELISA. Caspase-3 and caspase-9 levels in SW620 and HT29 cells were examined using caspase-3 (cat. no. ab39401; Abcam) and caspase-9 (cat. no. ab65608; Abcam) ELISA kits.

Wound healing assay. Serum-starved SW620 and HT29 cells were seeded onto a 6-well plate ($5x10^5$ cells/well) overnight. Cells were incubated at 37˚C until they reached 100% confluence. A 200-μl tip was used to scratch the plate. After removing the scratched cells, the 6-well plate was placed in a 5% CO_2 incubator at 37˚C. The images were observed under a light microscope (magnification, x100; Olympus Corporation) at 0 and 48 h. The migratory rate was measured by quantifying the total distance that cells migrated from the edge of the wound towards the center of the wound.

Transwell assay. Transwell inserts (Costar; Corning, Inc.) were incubated with 50 μl diluted Matrigel (BD Biosciences) at 37˚C for 1 h. Cells ($1x10^5$) were seeded onto the upper chamber of the Transwell insert with 600 μl medium without FBS. In the lower chamber of the Transwell plate, 600 μl medium with 10% FBS was added. After 48 h at 37˚C, the invaded cells were fixed with 4% paraformaldehyde at room temperature for 15 min and stained with 2% crystal violet staining solution at room temperature for 10 min. These results were investigated under an inverted microscope (magnification, x200). The non-invaded cells were wiped off and the number of cells passing through the Matrigel was counted. Cells in five random fields were counted using ImageJ software (version 1.8.0; National Institutes of Health).

Western blotting. SW620 and HT29 cells or tissues were lysed using RIPA lysis buffer (cat. no. P0013B; Beyotime Institute of Biotechnology) on ice. Protein concentration was detected

using a BCA detection kit (cat. no. P0009; Beyotime Institute of Biotechnology). Protein samples (20 μg) were subjected to 10% SDS-PAGE, and subsequently transferred onto PVDF membranes. The membrane was then blocked with 5% skimmed milk powder blocking solution at room temperature for 2 h, followed by incubation overnight at 4˚C with primary antibodies against N-cadherin (1:1,000; cat. no. ab76057; Abcam), vimentin (1:1,000; cat. no. 5741; Cell Signaling Technology, Inc.), S100A11 (1:1,000; cat. no. ab180593; Abcam), GAPDH (1:1,000; cat. no. ab181602, Abcam). Subsequently, membranes were incubated with secondary antibodies (1:1,000; cat. no. ab97080; Abcam) at room temperature for 1 h. The blots were visualized by an ECL kit (KGP1121; KeyGen Biotech Co., Ltd.). The optical density was measured with ImageJ software (version 1.8.0; National Institutes of Health).

Subcellular fractionation assay. According to the manufacturer's instructions, the cellular cytoplasmic and nuclei fractions were isolated using the Cytoplasmic & Nuclear RNA Purification kit (cat. no. 37400; Norgen Biotek Corp.). Cytoplasmic and nuclear LBX2-AS1 levels were detected via RT-qPCR.

Statistical analysis. SPSS 23.0 software (IBM Corp.) and GraphPad Prism 8.0 (GraphPad Software, Inc.) were used for statistical analyses. All data are presented as the mean ± standard deviation from at least three repeats. Comparisons between normal tissues and tumor tissues were analyzed using a paired Student's t-test. Other comparisons between two groups were analyzed using an unpaired Student's t-test. One-way ANOVA followed by post hoc Tukey's test was utilized to assess the differences between multiple groups. The differences in clinicopathological parameters between high and low LBX2-AS1 expression samples were analyzed using a Chi-squared test. Univariate and multivariate Cox regression analyses were conducted to analyze the association between LBX2-AS1 and patient prognosis. For survival analysis, 145 patients with colorectal cancer were stratified into high- and low-expression groups based on the median value of LBX2-AS1 expression. Kaplan-Meier survival curve and log-rank test were performed to assess the differences and OS and disease-free survival (DFS) time between high- and low-expression groups. A receiver operating characteristic (ROC) curve was plotted to validate the diagnostic efficacy of LBX2-AS1. $P<0.05$ was considered to indicate a statistically significant difference.

Results

LBX2-AS1 is a promising diagnostic and prognostic marker for patients with colorectal cancer. According to the microarray profile, LBX2-AS1 expression was higher in colorectal cancer tissues compared with that in normal tissues (Fig. 1A). Using the GEPIA database, it was found that there was a distinct difference in LBX2-AS1 expression between colorectal cancer tissues (n=349) and normal tissues (n=275), as presented in Fig. 1B. Moreover, LBX2-AS1 expression was upregulated among different clinical stages (Fig. 1C). In total, 145 patients with colorectal cancer were included in the present study. The results of RT-qPCR showed that LBX2-AS1 was significantly upregulated in colorectal cancer tissues (Fig. 1D). Furthermore, the differences in its expression between stage I-II and III-IV were determined. As shown in Fig. 1E, expression of LBX2-AS1 was higher at stage III-IV compared with stage I-II, indicating that it was associated with the severity of colorectal cancer. Also, compared with the human normal colorectal mucosa FHC cell line, LBX2-AS1 was significantly elevated in the four colorectal cancer cell lines (Fig. 1F). The ROC results suggested that LBX2-AS1 could possess a useful diagnostic function for the cohort of patients with colorectal cancer included in the present study (Fig. 1G). High LBX2-AS1 expression had a positive association with poorer OS (Fig. 1H), but not DFS (Fig. 1I), using data from TCGA database. The 145 patients with colorectal cancer from the present study were separated into high- and low-expression groups based on the cutoff of LBX2-AS1 expression. Consistently, high expression of LBX2-AS1 suggested shorter OS time (Fig. 1J) and poorer DFS (Fig. 1K). The association between LBX2-AS1 expression and clinicopathological features of patients with colorectal cancer was then calculated. Significant associations between the expression of LBX2-AS1 with lymph node metastasis and TNM stage were found, and are presented in Table II. After multivariate Cox regression analysis, LBX2-AS1 expression was found to be a potential independent prognostic factor for colorectal cancer (Table III). The aforementioned results suggested that LBX2-AS1 was elevated both in colorectal cancer tissues and cells, and could be a potential diagnostic and prognostic biomarker for patients with colorectal cancer.

Transcription factor ELK1 mediates the upregulation of LBX2-AS1 in colorectal cancer cells. To thoroughly explore the molecular mechanisms regarding the upregulation of LBX2-AS1 in colorectal cancer, 19 transcription factors that could bind to the promoter of LBX2-AS1 were predicted (Fig. 2A). Among them, ELK1 was upregulated in colorectal cancer samples in comparison with normal samples using TCGA database (Fig. 2B). In the patients with colorectal cancer included in the present study, ELK1 expression was significantly higher in colorectal cancer tissues in comparison with normal tissues (Fig. 2C). Moreover, higher ELK1 expression was found in colorectal cancer cells compared with in FHC cells (Fig. 2D). To observe whether ELK1 could mediate the expression of LBX2-AS1, two colorectal cancer cell lines, HT29 and SW620, which were chosen as they exhibited the lowest expression of LBX2-AS1 (Fig. 1F), were transfected with si-ELK1 and pcDNA-ELK1 (Fig. 2E). LBX2-AS1 expression was significantly downregulated in colorectal cancer cells transfected with si-ELK1 compared with those transfected with the si-NC. LBX2-AS1 expression was significantly higher in colorectal cancer cells transfected with pcDNA-ELK1 compared with the empty vector group (Fig. 2F). The RIP assay demonstrated that ELK1 could directly bind to the promoter region of LBX2-AS1 (Fig. 2G). As presented in Fig. 2H, the dual-luciferase reporter assay demonstrated that two binding sites (site 1, -437 ~ -405; site 2, -346 ~ -329) on the promoter region of LBX2-AS1 could be involved in transcriptional activation of ELK1. As expected, relative luciferase activity was significantly increased in colorectal cancer cells transfected with pcDNA-ELK1 compared with the empty vector

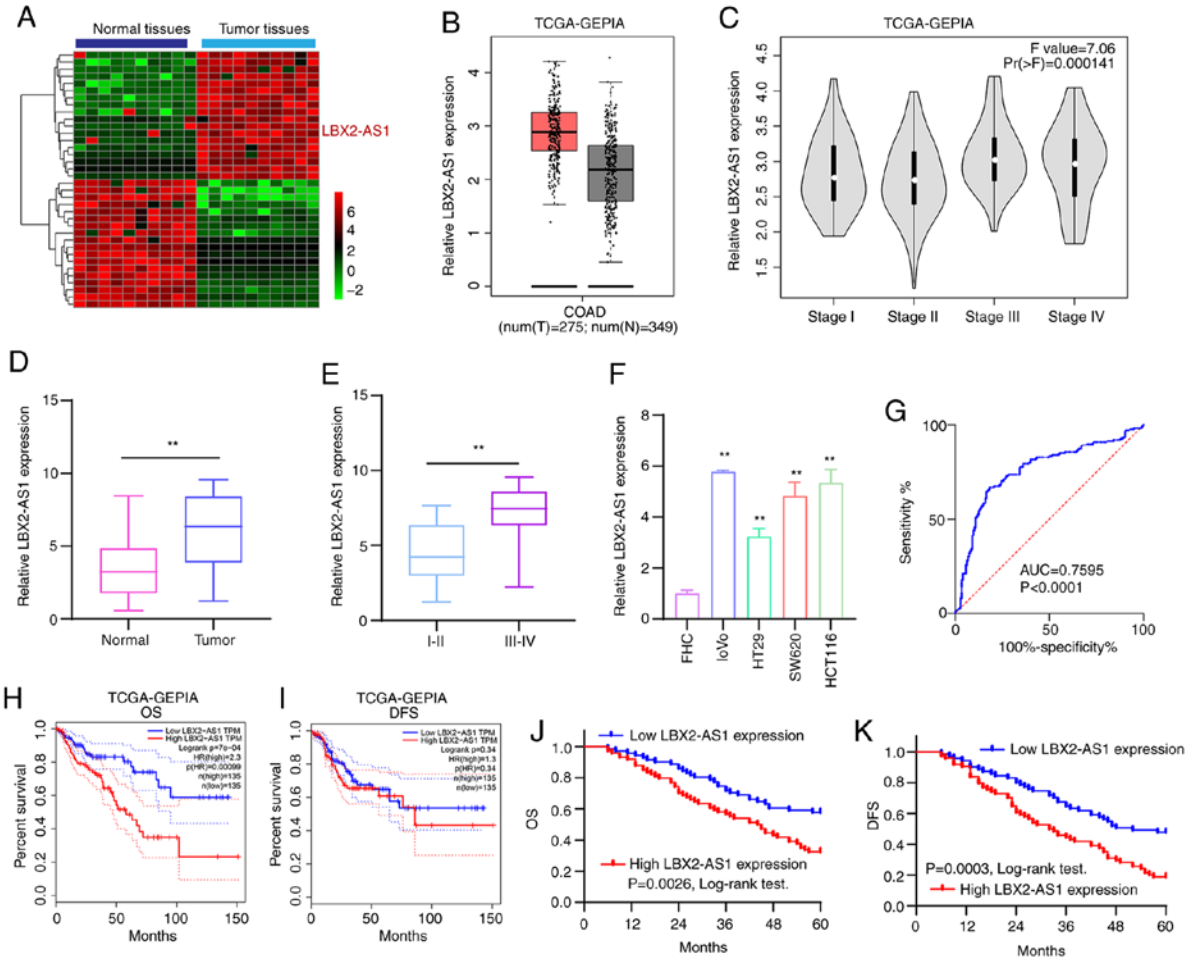

Figure 1. High LBX2-AS1 expression is a promising diagnostic and prognostic biomarker for patients with colorectal cancer. (A) Heatmap depicting aberrantly expressed lncRNAs between 10 pairs of colorectal cancer specimens and normal specimens. Red, upregulation; green, downregulation. (B) The difference in expression pattern of LBX2-AS1 between colorectal cancer samples and normal samples from TCGA database. (C) The difference in LBX2-AS1 expression among different clinical stages of colorectal cancer from TCGA database. (D) Box plots showing the expression levels of LBX2-AS1 between colorectal cancer and normal tissues from a total of 145 colorectal cancer cohort according to RT-qPCR. (E) Box plots showing the difference in LBX2-AS1 expression between stage III-IV and I-II. **P<0.01. (F) RT-qPCR results demonstrated high LBX2-AS1 expression in colorectal cancer cell lines. **P<0.01 vs. FHC cells. (G) AUC of receiver operating characteristic curve was 0.7595 and P<0.0001, indicating a high sensitivity and accuracy of LBX2-AS1 for colorectal cancer diagnosis. In TCGA database, LBX2-AS1 expression was associated with (H) OS, but not (I) DFS. (J and K) Among 145 patients with colorectal cancer, LBX2-AS1 expression had a positive association with poorer OS and DFS. LBX2-AS1, LBX2 antisense RNA 1; lncRNA, long non-coding RNA; TCGA, The Cancer Genome Atlas; RT-qPCR, reverse transcription-quantitative PCR; AUC, area under the curve; OS, overall survival; DFS, disease-free survival; GEPIA, Gene Expression Profiling Interactive Analysis.

group (Fig. 2I). After deletion of binding site 2 of LBX2-AS1, relative luciferase activity was also significantly increased in colorectal cancer cells transfected with pcDNA-ELK1 compared with the empty vector group. However, after deletion of binding site 1 of LBX2-AS1, pcDNA-ELK1 did not change the luciferase activity compared with the empty vector group (Fig. 2I). Furthermore, it was found that relative luciferase activity was significantly decreased in colorectal cancer cells transfected with si-ELK1 compared with si-NC group (Fig. 2J). These findings revealed that ELK1 could induce LBX2-AS1 upregulation in colorectal cancer cells.

Suppression of LBX2-AS1 inhibits colorectal cancer cell proliferation and promotes apoptosis. Two siRNAs against LBX2-AS1 were synthesized and transfected into HT29 and SW620 cells. RT-qPCR results verified that LBX2-AS1 was efficiently silenced in cells (Fig. 3A). According to CCK-8 assay results, si-LBX2-AS1 significantly suppressed the viability of colorectal cancer cells (Fig. 3B). Furthermore, the clone formation ability of HT29 or SW620 colorectal cancer cells was significantly suppressed after transfection with si-LBX2-AS1 (Fig. 3C). As shown in Fig. 3D, si-LBX2-AS1 significantly promoted the apoptosis of colorectal cancer cells. Following transfection with si-LBX2-AS1, caspase-3 and caspase-9 levels were significantly higher compared with the si-NC group (Fig. 3E). Therefore, these findings suggested that suppression of LBX2-AS1 may inhibit proliferation and induce apoptosis in colorectal cancer cells.

Silencing LBX2-AS1 suppresses migration, invasion and epithelial-mesenchymal transition (EMT) in colorectal cancer cells. After silencing LBX2-AS1 expression, the migratory ability of HT29 and SW620 cells was significantly suppressed (Fig. 4A and B). Furthermore, the number of invasive cells was significantly lower in colorectal cancer cells transfected with si-LBX2-AS1 (Fig. 4C). Additionally, the

Table II. Association between LBX2-AS1 expression and clinicopathological features of patients with colorectal cancer.

Parameters	Total, n	LBX2-AS1 expression, n		P-value
		High	Low	
Sex				0.949
Male	78	40	38	
Female	67	34	33	
Age, years				0.737
<60	71	37	34	
≥60	75	37	38	
Tumor size, cm				0.207
<5	92	43	49	
≥5	52	30	22	
Lymph node metastasis				0.011[a]
Negative	109	49	60	
Positive	36	25	11	
TNM stage				0.028[a]
I-II	102	46	56	
III-IV	43	28	15	

[a]P<0.05. LBX2-AS1, LBX2 antisense RNA 1; TNM, tumor node metastasis.

Table III. Multivariate Cox regression analysis of clinicopathological features and LBX2-AS1 expression in the prognosis of patients with colorectal cancer.

A, Overall survival

Variables	HR	95% CI	P-value
Sex	1.223	0.643-2.173	0.361
Age, years	1.462	0.783-2.018	0.218
Tumor size, cm	1.656	0.827-2.218	0.187
Lymph node metastasis	3.017	1.216-4.775	0.021[a]
TNM stage	2.896	1.385-4.452	0.027[a]
LBX2-AS1 expression	3.163	1.375-4.882	0.015[a]

B, Disease-free survival

Variables	HR	95% CI	P-value
Sex	1.364	0.732-2.018	0.168
Age, years	1.271	0.832-2.217	0.185
Tumor size, cm	1.327	0.562-2.326	0.125
Lymph node metastasis	3.256	1.317-4.882	0.009[b]
TNM stage	3.017	1.462-4.776	0.011[a]
LBX2-AS1 expression	3.325	1.426-5.127	0.003[b]

[a]P<0.05; [b]P<0.01. LBX2-AS1, LBX2 antisense RNA 1; TNM, tumor node metastasis; HZ, hazard ratio; CI, confidence interval.

expression of EMT-related proteins in colorectal cancer cells was investigated. As expected, western blotting results showed that N-cadherin and vimentin protein expression was reduced in HT29 and SW620 cells transfected with si-LBX2-AS1 (Fig. 4D and E), indicating that the EMT process of colorectal cancer cells was blocked after silencing LBX2-AS1.

LBX2-AS1 serves as a sponge of hsa-miR-491-5p in colorectal cancer cells. LBX2-AS1 was mainly distributed in the nucleus and cytoplasm (Fig. 5A and B). In HT29 and SW620 colorectal cancer cells, LBX2-AS1 expression was detected in the nucleus and cytoplasm (Fig. 5C), which was consistent with the prediction results. Using the starBase database, potential target miRNAs of LBX2-AS1 were predicted. To observe which miRNAs could directly bind to LBX2-AS1, dual-luciferase reporter assays were performed after LBX2-AS1 wild-type was co-transfected with NC, miR-3174 mimics, miR-627-5p mimics, miR-151b mimics, miR-627-5b mimic, miR-491-5p mimics or miR-650 mimics. The results confirmed that only hsa-miR-491-5p mimics and LBX2-AS1 wild-type co-transfection could significantly reduce relative luciferase levels (Fig. 5D and E). LBX2-AS1 was weakly negatively correlated with hsa-miR-491-5p in 450 cases of colorectal cancer specimens from the starBase database (Fig. 5F). The RT-qPCR results demonstrated that hsa-miR-491-5p expression was decreased in colorectal cancer tissues (Fig. 5G) and cells (Fig. 5H). As expected, there was a moderate negative correlation between hsa-miR-491-5p and LBX2-AS1 expression, which was validated among 145 patients with colorectal cancer included in the present study (Fig. 5I). To observe the regulatory mechanisms of hsa-miR-491-5p, hsa-miR-491-5p was successfully overexpressed by miR-491-5p mimics (Fig. 5J). Dual-luciferase reporter results confirmed that, when miR-491-5p mimics and LBX2-AS1-WT were co-transfected into cells, relative luciferase activity was significantly decreased (Fig. 5K). Furthermore, after transfection with si-LBX2-AS1, hsa-miR-491-5p expression was significantly elevated in two colorectal cancer cells (Fig. 5L). Conversely, LBX2-AS1 expression was significantly suppressed in cells transfected with miR-491-5p mimics (Fig. 5M). Thus, LBX2-AS1 may serve as a sponge of hsa-miR-491-5p in colorectal cancer cells.

S100A11 is highly expressed in colorectal cancer and acts as a potential target of miR-491-5p. The heatmap presented in Fig. 6A shows the differences in expression patterns of the top 25 DEGs between colorectal cancer and normal tissues. Also, these genes were visualized into volcano plots (Fig. 6B). Among them, S100A11 was highly expressed both in TCGA database (Fig. 6C) and TCGA/GTEx database (Fig. 6D). Furthermore, there was a difference in S100A11 expression among different clinical stages (Fig. 6E). From the UALCAN database, high S100A11 expression was found in colorectal cancer using data from the CPTAC dataset (Fig. 6F). In addition, hsa-miR-491-5p was weakly correlated with S100A11 in a dataset from the starBase database (Fig. 6G). S100A11 was highly expressed in a number of cancer types, except colorectal cancer (Fig. 6H). Results of RT-qPCR confirmed that S100A11 expression was

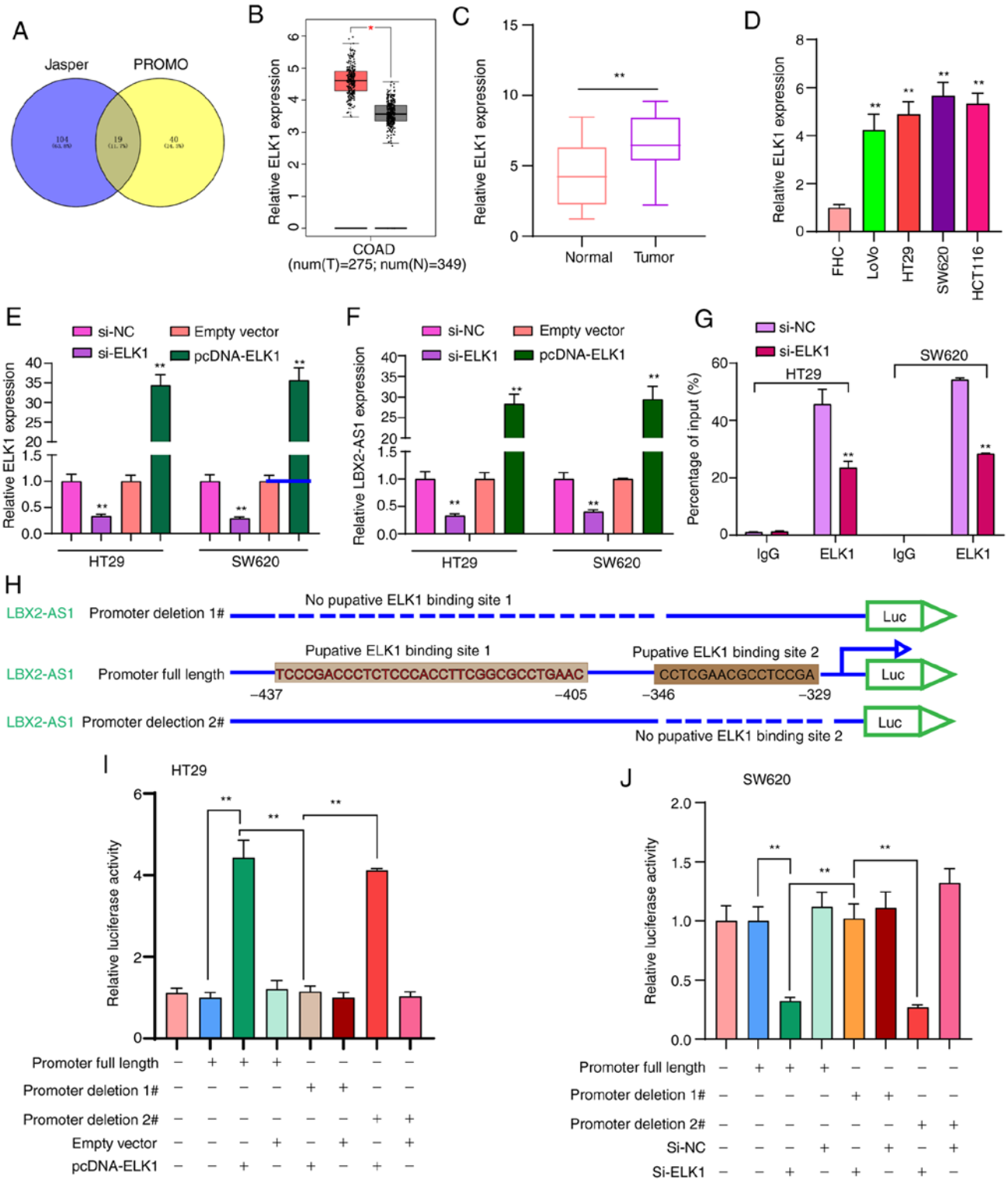

Figure 2. ELK1 induces LBX2-AS1 upregulation in colorectal cancer cells. (A) A total of 19 transcription factors were predicted for LBX2-AS1 using the JASPAR and PROMO databases. (B) Differentially expressed transcription factor ELK1 was found in colorectal cancer according to The Cancer Genome Atlas database. *P<0.05. (C) High ELK1 expression was validated in a cohort of 145 patients with colorectal cancer using RT-qPCR. **P<0.01. (D) ELK1 mRNA was elevated in four colorectal cancer cell lines, as determined via RT-qPCR. **P<0.01 vs. FHC cells. (E) ELK1 was silenced or overexpressed in HT29 and SW620 colorectal cancer cells. (F) RT-qPCR results suggested that LBX2-AS1 expression was inhibited after ELK1 knockdown and was elevated after transfection with pcDNA-ELK1 in colorectal cancer cells. (G) RNA immunoprecipitation assay results confirmed that ELK1 directly bound to the promoter region of LBX2-AS1. **P<0.01 vs. si-NC or empty vector. (H) Two binding sites on the promoter region of LBX2-AS1 for ELK1. (I and J) The relative luciferase activity was measured after deletion of two binding sites of LBX2-AS1 for ELK1 in HT29 and SW620 colorectal cancer cells. **P<0.01. ELK1, ETS transcription factor ELK1; LBX2-AS1, LBX2 antisense RNA 1; RT-qPCR, reverse transcription-quantitative PCR; si-, small interfering RNA; NC, negative control.

higher in colorectal cancer tissues (Fig. 6I) and cells (Fig. 6J). As shown in the bioinformatics analysis, miR-491-5p could bind to the 3'UTR region of S100A11 (Fig. 6K). In both HT29 and SW620 cells, co-transfection of S100A11-WT and miR-491-5p

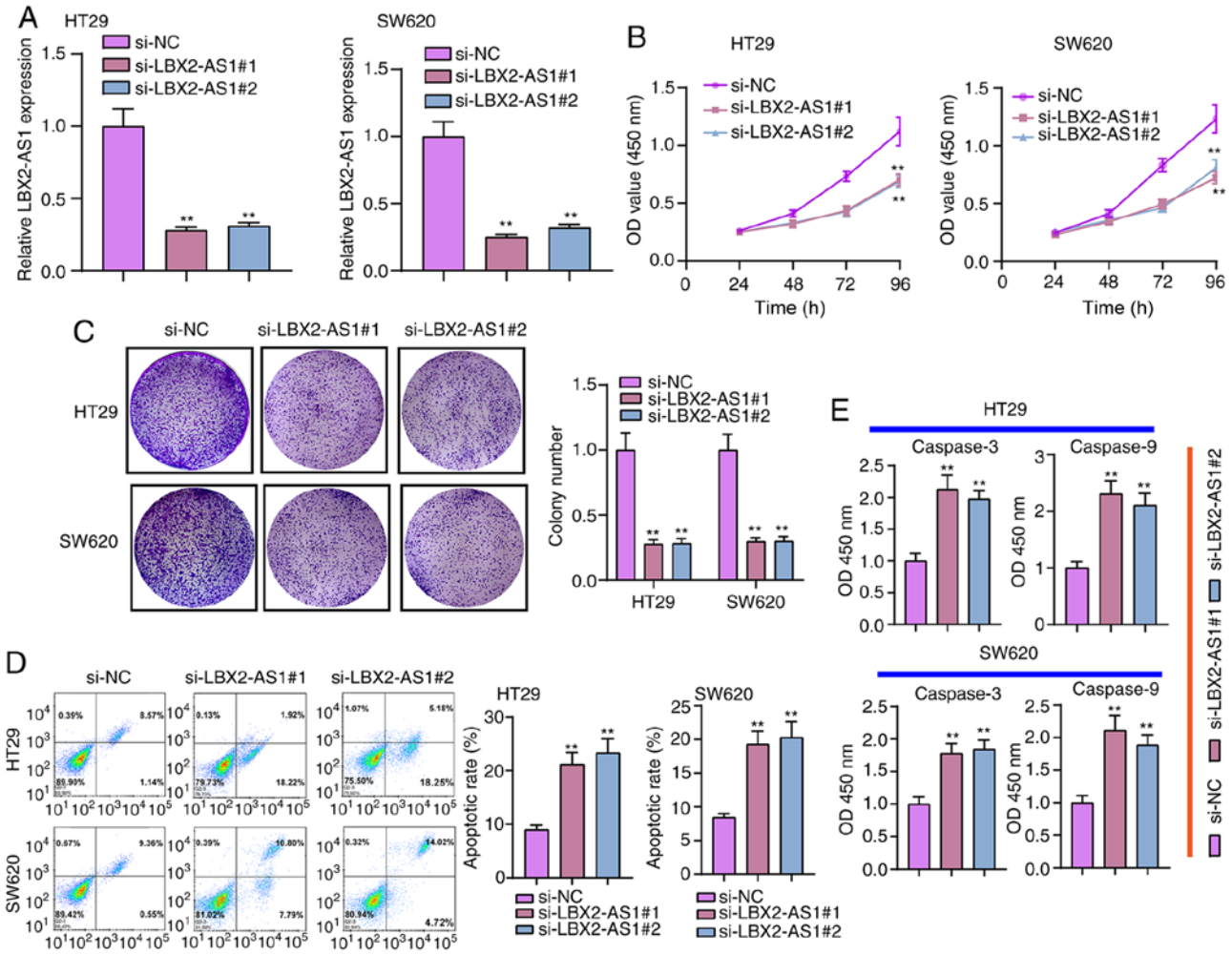

Figure 3. Suppression of LBX2-AS1 inhibits proliferation and increases apoptosis of colorectal cancer cells. (A) LBX2-AS1 was silenced in HT29 and SW620 colorectal cancer cells following transfection with si-LBX2-AS1#1 or #2. (B) Cell Counting Kit-8 assay results showed that cell viability was inhibited in colorectal cancer cells transfected with si-LBX2-AS1. (C) The inhibitory effect of silencing LBX2-AS1 on colony formation was investigated in two colorectal cancer cells. (D) Flow cytometry assay results confirmed that the apoptosis of colorectal cancer cells was induced by si-LBX2-AS1. (E) Higher caspase-3 and caspase-9 expression levels were detected in colorectal cancer cells transfected with si-LBX2-AS1. **P<0.01 vs. si-NC. LBX2-AS1, LBX2 antisense RNA 1; si-, small interfering RNA; NC, negative control.

mimics significantly reduced the relative luciferase activity (Fig. 6L). After miR-491-5p overexpression with mimics, S100A11 expression was significantly reduced in colorectal cancer cells (Fig. 6M). Therefore, S100A11 could act as a target of miR-491-5p in colorectal cancer.

LBX2-AS1 promotes colorectal cancer cell proliferation and invasion by mediating the miR-491-5p/S100A11 axis. RT-qPCR results confirmed that LBX2-AS1 was successfully overexpressed in HT29 and SW620 cells transfected with pcDNA-LBX2-AS1 (Fig. 7A). The mRNA expression of S100A11 was significantly downregulated in HT29 and SW620 cells transfected with si-LBX2-AS1, as determined via RT-qPCR (Fig. 7B). On the other hand, transfection with pcDNA-LBX2-AS1 significantly promoted S100A11 mRNA expression in colorectal cancer cells (Fig. 7B). At the protein level, in two colorectal cancer cells transfected with pcDNA-LBX2-AS1, S100A11 expression was significantly elevated (Fig. 7C and D). However, transfection with miR-491-5p mimics significantly decreased the expression of S100A11 protein in cells. Of note, LBX2-AS1 overexpression could reverse the inhibitory effects of transfection with miR-491-5p mimics on S100A11 protein expression (Fig. 7C and D), indicating that LBX2-AS1 may indirectly enhance the mRNA expression of S100A11 via blocking miR-491-5p. As expected, the repressive functions of miR-491-5p mimics on cell viability were found in HT29 and SW620 cells, as determined via a CCK-8 assay, which were ameliorated by transfection with pcDNA-LBX2-AS1 (Fig. 7E). In the colony formation assay, the colony number of HT29 and SW620 cells was significantly reduced following transfection with miR-491-5p mimics (Fig. 7F). Nonetheless, after co-transfection of miR-491-5p mimics and pcDNA-LBX2-AS1, the colony formation ability of colorectal cancer cells was significantly enhanced compared with the miR-491-5p mimics group (Fig. 7F). Moreover, LBX2-AS1 overexpression was capable of partially reversing the suppressive effect of miR-491-5p mimics on colorectal cancer cell invasion (Fig. 7G). The aforementioned findings suggested that LBX2-AS1 could enhance colorectal cancer cell proliferation and invasion via regulation of the miR-491-5p/S100A11 axis.

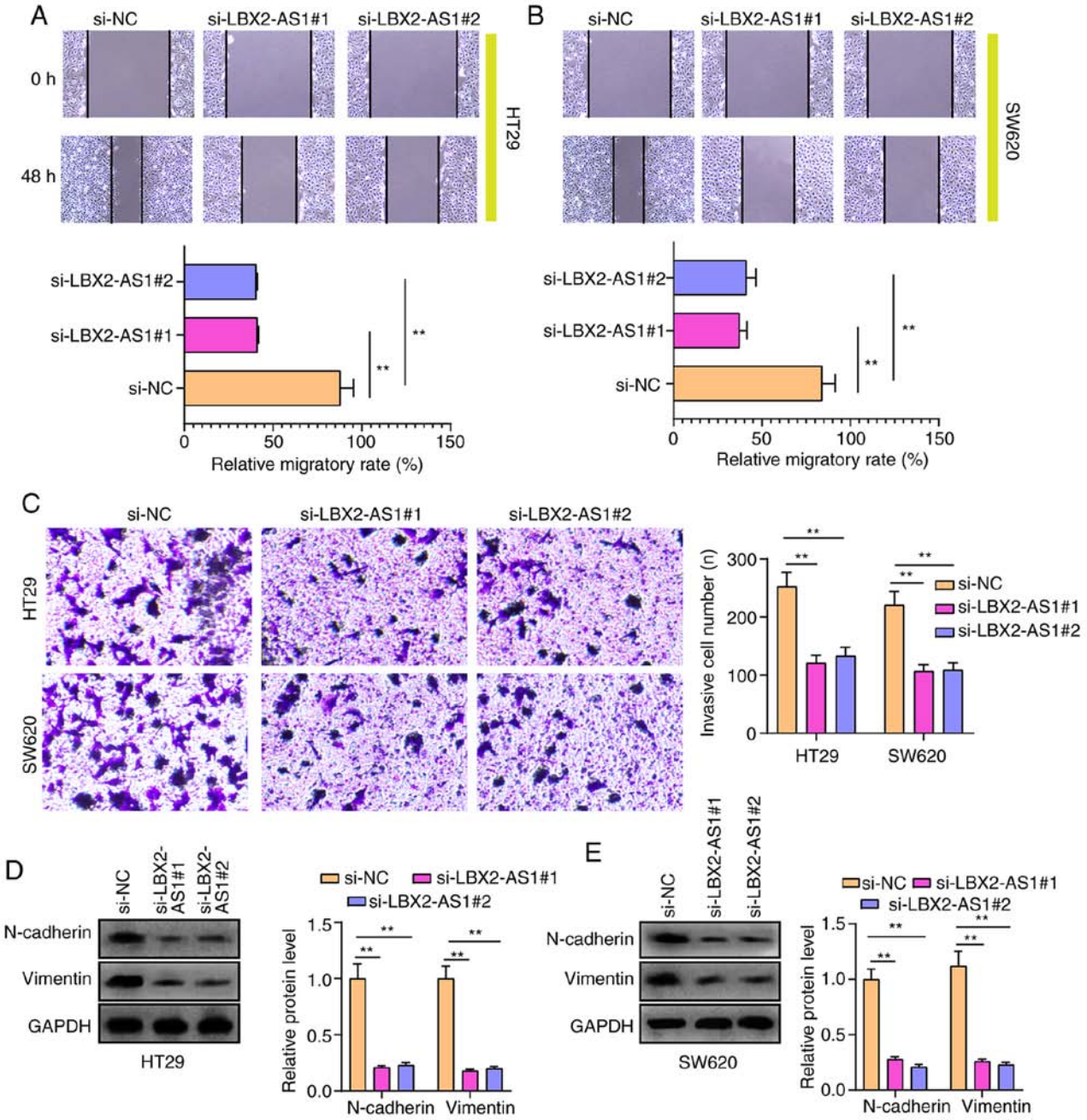

Figure 4. Silencing LBX2-AS1 suppresses migration, invasion and EMT in colorectal cancer cells. (A and B) Wound healing assay showed the inhibitory effects of si-LBX2-AS1 on the migratory ability of HT29 and SW620 cells. (C) According to the Transwell assay, the number of invasive cells was lower after silencing LBX2-AS1. (D and E) EMT-related proteins, including N-cadherin and Vimentin, were detected via western blotting in cells transfected with si-LBX2-AS1. **P<0.01. LBX2-AS1, LBX2 antisense RNA 1; si-, small interfering RNA; NC, negative control; EMT, epithelial-mesenchymal transition.

Discussion

The present study identified a novel finding that lncRNA LBX2-AS1 could be a potential underlying diagnostic and prognostic marker for colorectal cancer. Mechanically, LBX2-AS1, induced by transcription factor ELK1, facilitates cell proliferation, migration and invasion via the mediation of the miR-491-5p/S100A11 axis in colorectal cancer cells.

High LBX2-AS1 expression was found in both colorectal cancer tissues and cells. Previously, LBX2-AS1 expression has been verified to be elevated in several types of cancer (11,13). The ROC results of the present study demonstrated that LBX2-AS1 was a sensitive diagnostic marker in patients with colorectal cancer. In colorectal cancer, high LBX2-AS1 expression predicted poor clinical outcomes. Furthermore, LBX2-AS1 expression was associated with the clinical stages of colorectal cancer. Patients diagnosed as stage III-IV usually had higher LBX2-AS1 expression than those with stage I-II. Previous studies have confirmed that upregulated LBX2-AS1 expression is associated with unfavorable prognosis of lung carcinoma (12), stomach carcinoma (13) and liver cancer (14). In the present study, multivariate Cox regression analysis showed that LBX2-AS1 expression could be an independent prognostic factor for colorectal cancer.

In the current study, transcription factor ELK1 was notably upregulated in colorectal cancer tissues, as well as

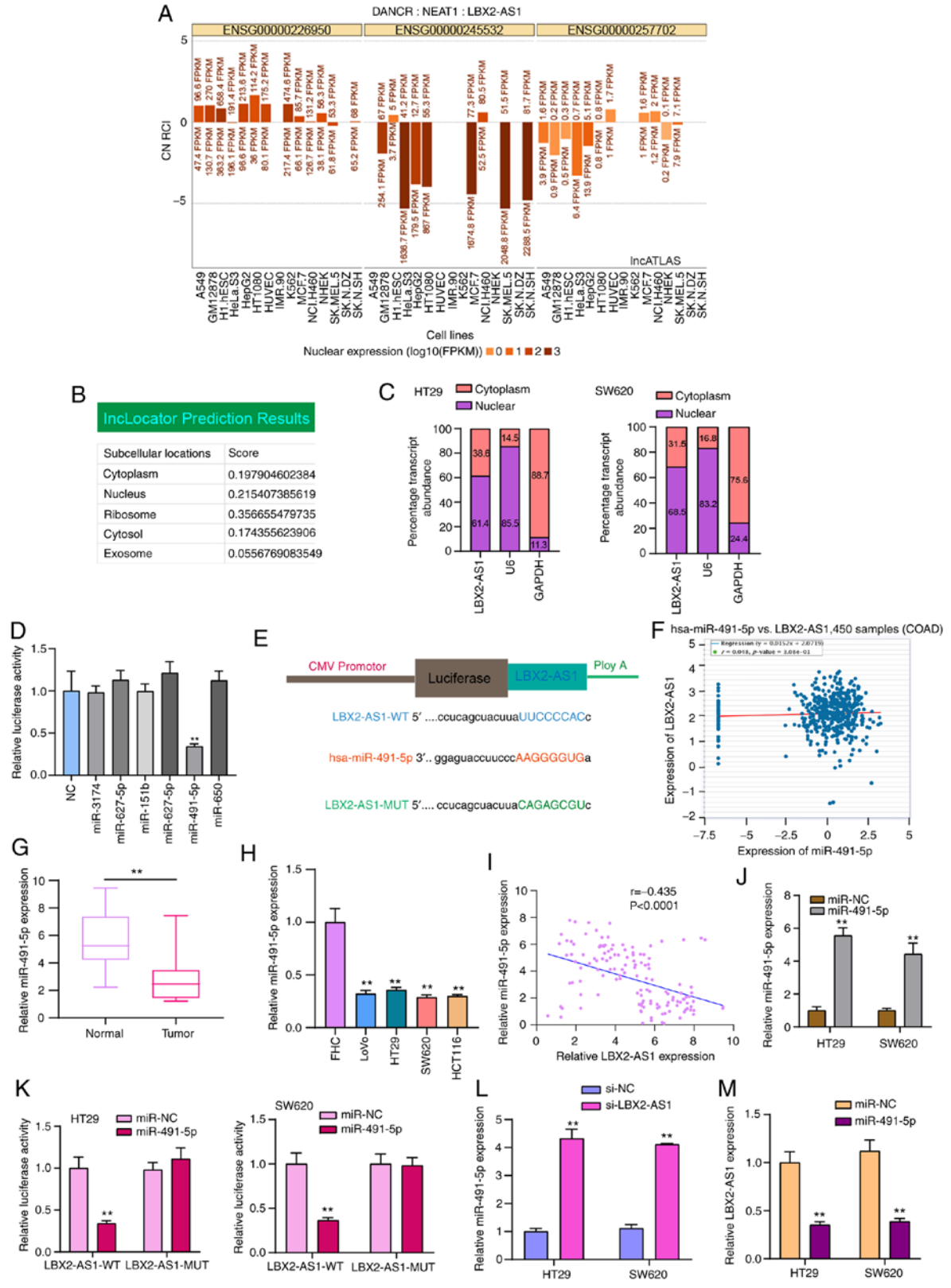

Figure 5. LBX2-AS1 serves as a sponge of hsa-miR-491-5p in colorectal cancer cells. (A and B) Subcellular locations of LBX2-AS1 were predicted using the lncATLAS and lncLocator databases. (C) Subcellular locations of LBX2-AS1 were determined in HT29 and SW620 colorectal cancer cells. (D) Dual-luciferase reporter assay showed that there was a direct target relationship between hsa-miR-491-5p and LBX2-AS1. **P<0.01 vs. NC. (E) Schematic diagram of the binding site of hsa-miR-491-5p and LBX2-AS1. (F) A weak negative correlation was found between hsa-miR-491-5p and LBX2-AS1, which was identified from the starBase database. (G and H) miR-491-5p expression was decreased in colorectal cancer tissues and cells, as determined via RT-qPCR. **P<0.01 vs. normal tissues or FHC cells. (I) There was a moderate negative correlation between LBX2-AS1 and miR-491-5p in a cohort of 145 patients with colorectal cancer (r=-0.4345, P<0.0001). (J) miR-491-5p expression was determined in colorectal cancer cells transfected with miR-491-5p mimics via RT-qPCR. (K) Dual-luciferase reporter assay confirmed that LBX2-AS1 could act as a sponge of hsa-miR-491-5p in colorectal cancer cells. (L) miR-491-5p expression was determined in colorectal cancer cells transfected with si-LBX2-AS1 via RT-qPCR. (M) The relative LBX2-AS1 expression was quantified in colorectal cancer cells following transfection with miR-491-5p mimics, as determined via RT-qPCR. **P<0.01 vs. miR-NC or si-NC. LBX2-AS1, LBX2 antisense RNA 1; si-, small interfering RNA; NC, negative control; miR, microRNA; RT-qPCR, reverse transcription-quantitative PCR; WT, wild-type; MUT, mutant.

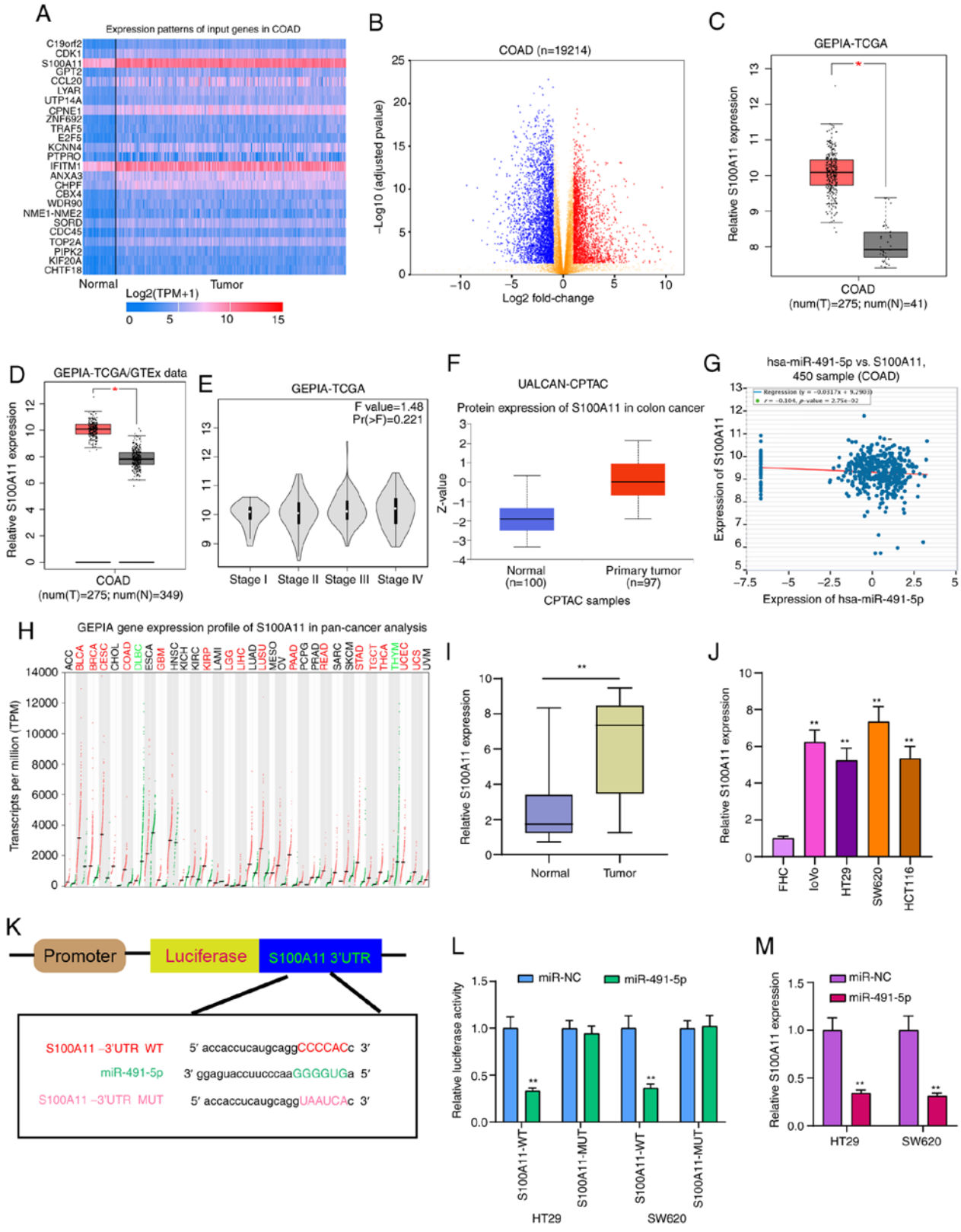

Figure 6. S100A11 is highly expressed in colorectal cancer tissues and cells, and acts as a potential target for miR-491-5p. (A) Heatmap showing the top 25 DEGs between colorectal cancer and normal samples in TCGA database. (B) All DEGs were visualized in volcano plots. (C and D) High S100A11 expression was found in colorectal cancer from TCGA database and TCGA/GTEx database. *P<0.05. (E) Violin plots showing the expression pattern of S100A11 in different colorectal cancer stages. (F) Box plots depicting the high S100A11 expression in colorectal cancer from the UALCAN database. (G) There was a weak negative correlation between S100A11 and miR-491-5p, which was identified from the starBase database. (H) The expression patterns of S100A11 in a pan-cancer analysis. (I and J) S100A11 expression was verified in colorectal cancer tissues and cells via reverse transcription-quantitative PCR. **P<0.01 vs. normal tissues or FHC cells. (K) Schematic diagram of the binding site between hsa-miR-491-5p and S100A11. (L) Dual-luciferase reporter assay results confirmed that miR-491-5p directly bound to the 3'UTR region of S100A11. (M) S100A11 expression was detected in colorectal cancer cells following transfection with miR-491-5p mimics. **P<0.01 vs. miR-NC. miR, microRNA; NC, negative control; DEGs, differentially expressed genes; TCGA, The Cancer Genome Atlas; GTEx, The Genotype-Tissue Expression project; COAD, colon adenocarcinoma; GEPIA, Gene Expression Profiling Interactive Analysis; CPTAC, Clinical Proteomic Tumor Analysis Consortium; WT, wild-type; MUT, mutant.

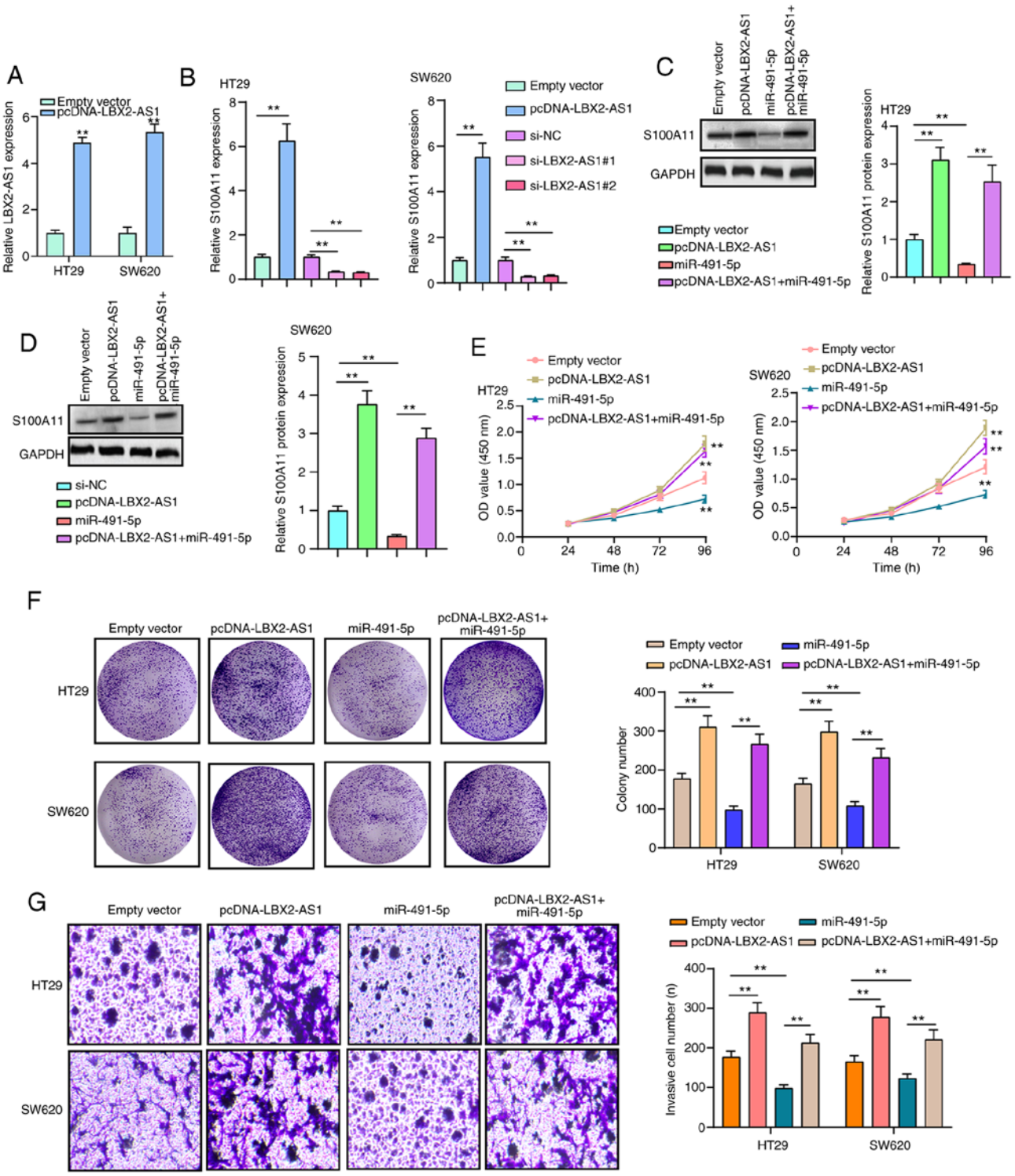

Figure 7. LBX2-AS1 promotes colorectal cancer cell proliferation and invasion via mediating the miR-491-5p/S100A11 axis. (A) The expression of LBX2-AS1 was assessed in HT29 and SW620 cells transfected with pcDNA-LBX2-AS1 via RT-qPCR. **P<0.01 vs. empty vector. (B) The expression of S100A11 mRNA was determined in HT29 and SW620 cells transfected with pcDNA-LBX2-AS1 or si-LBX2-AS1 via RT-qPCR. **P<0.01. (C and D) The expression of S100A11 protein was measured in HT29 and SW620 cells transfected with pcDNA-LBX2-AS1 and/or miR-491-5p mimics according to western blotting. **P<0.01. (E) The cell viability of HT29 and SW620 cells was determined via a Cell Counting Kit-8 assay after transfection with pcDNA-LBX2-AS1 and/or miR-491-5p mimics. **P<0.01 vs. empty vector. (F) Clone formation and (G) invasive ability of HT29 and SW620 cells were assessed after transfection with pcDNA-LBX2-AS1 and/or miR-491-5p mimics. **P<0.01. LBX2-AS1, LBX2 antisense RNA 1; miR, microRNA; NC, negative control; RT-qPCR, reverse transcription-quantitative PCR; si-, small interfering RNA.

cells, which was consistent with previous studies (30-32). It has been confirmed that ELK1 overexpression promotes migration and invasion of colorectal cancer cells (31). Also, its upregulation facilitates proliferation and angiogenesis (30), and suppresses apoptosis in colorectal cancer cells (32). These findings demonstrate that ELK1 is likely to be involved in colorectal cancer progression. The results of the RIP and dual-luciferase reporter assays in the

present study verified that ELK1 could directly bind to the two conservative sites (located at -437/-405 and -346/-329) in the promoter region of LBX2-AS1. Therefore, LBX2-AS1 could act as a transcriptional target of ELK1. ELK1 has been confirmed to directly interact with the endogenous miR-31 promoter in a MAPK-dependent manner (33). The current study found that suppression of LBX2-AS1 could promote apoptosis of colorectal cancer cells. Moreover, silencing LBX2-AS1 could suppress proliferation, migration, invasion and EMT process in colorectal cancer cells. EMT is the key mechanism of tumor invasion and metastasis for colorectal cancer. Zinc finger E-box-binding homeobox 1-induced LBX2-AS1 upregulation promotes migration, invasion and EMT in esophageal cancer cells (11). Nuclear factor 1 C-type-mediated LBX2-AS1 enhances cellular proliferation, migration and invasion in gastric cancer (34). The findings of the present study demonstrated that LBX2-AS1 was distributed in the nucleus and cytoplasm of colorectal cancer cells. Low miR-491-5p expression was detected in colorectal cancer tissues and cells, which was consistent with a previous study (35). Furthermore, downregulation of miR-491-5p is associated with unfavorable prognosis in patients with colorectal cancer (36). Furthermore, low miR-491-5p expression can promote colorectal cancer cell proliferation (36). Circulating miR-491-5p can be used to distinguish patients with colorectal cancer from patients with adenoma (36). Dual-luciferase reporter results of the present study confirmed that LBX2-AS1 may play a role as a sponge of hsa-miR-491-5p in colorectal cancer cells.

Upregulation of S100A11 was found in colorectal cancer tissues and cells via RT-qPCR in the current study, as reported in previous studies (37-39). S100A11 is closely related to the EMT and invasive phenotypes of colorectal cancer cells (40,41). As shown in the dual-luciferase reporter assays performed in the present study, miR-491-5p may bind to the 3'UTR region of S100A11. Also, overexpression of miR-491-5p significantly reduced S100A11 expression in two colorectal cancer cells. Thus, S100A11 may serve as a target of miR-491-5p in colorectal cancer. Additionally, overexpression of LBX2-AS induced the upregulation of S100A11 at the mRNA and protein levels in colorectal cancer cells. More importantly, LBX2-AS1 may indirectly enhance the mRNA expression of S100A11 through blocking miR-491-5p. Furthermore, the suppressive effects of miR-491-5p mimics were notably reversed by LBX2-AS1 overexpression on colorectal cancer cell proliferation and invasion. Hence, these findings revealed that LBX2-AS1 could enhance colorectal cancer cell proliferation and invasion by means of mediating the miR-491-5p/S100A11 axis.

To conclude, in the present study, lncRNA LBX2-AS1 was identified to be upregulated in colorectal cancer, which was transcriptionally regulated by transcription factor ELK1. LBX2-AS1 could become a hopeful diagnostic and prognostic marker for colorectal cancer. It was further found that LBX2-AS1 overexpression facilitated cell proliferation, EMT, migration and invasion in colorectal cancer cells. LBX2-AS1 could block S100A11 degradation via competitively binding to miR-491-5p, thereby enhancing colorectal cancer development. Thus, these findings revealed the possible value of LBX2-AS1 in the diagnosis prognosis, and treatment of colorectal cancer.

Acknowledgements

Not applicable.

Funding

No funding was received.

Availability of data and materials

The datasets used and/or analyzed during the current study are available from the corresponding author on reasonable request.

Authors' contributions

XY conceived and designed the study. GM, WD and JZ conducted most of the experiments and data analysis, and wrote the manuscript. QL, BG and YS participated in data collection and helped to draft the manuscript. All authors read and approved the final manuscript. XY and GM confirm the authenticity of all the raw data.

Ethics approval and consent to participate

The present study was approved by the Ethics Committee of The Affiliated Huai'an No. 1 People's Hospital of Nanjing Medical University (approval no. 2014059; Huai'an, China). All subjects provided signed informed consent.

Patient consent for publication

Not applicable.

Competing interests

The authors declare that they have no competing interests.

References

1. Siegel RL, Miller KD and Jemal A: Cancer statistics, 2019. CA Cancer J Clin 69: 7-34, 2019.
2. Bekaii-Saab TS, Ou FS, Ahn DH, Boland PM, Ciombor KK, Heying EN, Dockter TJ, Jacobs NL, Pasche BC, Cleary JM, *et al*: Regorafenib dose-optimisation in patients with refractory metastatic colorectal cancer (ReDOS): A randomised, multicentre, open-label, phase 2 study. Lancet Oncol 20: 1070-1082, 2019.
3. Gunjur A: Targeted therapy for BRAF-mutant colorectal cancer. Lancet Oncol 20: e618, 2019.
4. Pfeiffer P, Yilmaz M, Möller S, Zitnjak D, Krogh M, Petersen LN, Poulsen LØ, Winther SB, Thomsen KG and Qvortrup C: TAS-102 with or without bevacizumab in patients with chemorefractory metastatic colorectal cancer: An investigator-initiated, open-label, randomised, phase 2 trial. Lancet Oncol 21: 412-420, 2020.
5. Hu M, Zhou X, Wang Y, Guan K and Huang L: Relaxin-FOLFOX-IL-12 triple combination therapy engages memory response and achieves long-term survival in colorectal cancer liver metastasis. J Control Release 319: 213-221, 2020.
6. Huyghe JR, Bien SA, Harrison TA, Kang HM, Chen S, Schmit SL, Conti DV, Qu C, Jeon J, Edlund CK, *et al*: Discovery of common and rare genetic risk variants for colorectal cancer. Nat Genet 51: 76-87, 2019.
7. Chi Y, Wang D, Wang J, Yu W and Yang J: Long non-coding RNA in the pathogenesis of cancers. Cells 8: 1015, 2019.
8. Galamb O, Barták BK, Kalmár A, Nagy ZB, Szigeti KA, Tulassay Z, Igaz P and Molnár B: Diagnostic and prognostic potential of tissue and circulating long non-coding RNAs in colorectal tumors. World J Gastroenterol 25: 5026-5048, 2019.

9. Wei L, Wang X, Lv L, Zheng Y, Zhang N and Yang M: The emerging role of noncoding RNAs in colorectal cancer chemoresistance. Cell Oncol (Dordr) 42: 757-768, 2019.
10. Xu M, Xu X, Pan B, Chen X, Lin K, Zeng K, Liu X, Xu T, Sun L, Qin J, *et al*: LncRNA SATB2-AS1 inhibits tumor metastasis and affects the tumor immune cell microenvironment in colorectal cancer by regulating SATB2. Mol Cancer 18: 135, 2019.
11. Zhang Y, Chen W, Pan T, Wang H, Zhang Y and Li C: LBX2-AS1 is activated by ZEB1 and promotes the development of esophageal squamous cell carcinoma by interacting with HNRNPC to enhance the stability of ZEB1 and ZEB2 mRNAs. Biochem Biophys Res Commun 511: 566-572, 2019.
12. Tang LX, Su SF, Wan Q, He P, Xhang Y and Cheng XM: Novel long non-coding RNA LBX2-AS1 indicates poor prognosis and promotes cell proliferation and metastasis through notch signaling in non-small cell lung cancer. Eur Rev Med Pharmacol Sci 23: 7419-7429, 2019.
13. Yang Z, Dong X, Pu M, Yang H, Chang W, Ji F, Liu T, Wei C, Zhang X and Qiu X: LBX2-AS1/miR-219a-2-3p/FUS/LBX2 positive feedback loop contributes to the proliferation of gastric cancer. Gastric Cancer 23: 449-463, 2020.
14. Wang Y, Zhao Y, Zhang X, Zhang A and Ma J: Long noncoding RNA LBX2-AS1 drives the progression of hepatocellular carcinoma by sponging microRNA-384 and thereby positively regulating IRS1 expression. Pathol Res Pract 216: 152903, 2020.
15. Sakai S, Ohhata T, Kitagawa K, Uchida C, Aoshima T, Niida H, Suzuki T, Inoue Y, Miyazawa K and Kitagawa M: Long noncoding RNA ELIT-1 acts as a Smad3 cofactor to facilitate TGFβ/Smad signaling and promote epithelial-mesenchymal transition. Cancer Res 79: 2821-2838, 2019.
16. Wang C, Yang Y, Zhang G, Li J, Wu X, Ma X, Shan G and Mei Y: Long noncoding RNA EMS connects c-Myc to cell cycle control and tumorigenesis. Proc Natl Acad Sci USA 116: 14620-14629, 2019.
17. Xie JJ, Jiang YY, Jiang Y, Li CQ, Lim MC, An O, Mayakonda A, Ding LW, Long L, Sun C, *et al*: Super-enhancer-driven long non-coding RNA LINC01503, regulated by TP63, is over-expressed and oncogenic in squamous cell carcinoma. Gastroenterology 154: 2137-2151.e1, 2018.
18. Cheng C, Zhang Z, Cheng F and Shao Z: Exosomal lncRNA RAMP2-AS1 derived from chondrosarcoma cells promotes angiogenesis through miR-2355-5p/VEGFR2 axis. Onco Targets Ther 13: 3291-3301, 2020.
19. Li P, Li Y, Dai Y, Wang B, Li L, Jiang B, Wu P and Xu J: The LncRNA H19/miR-1-3p/CCL2 axis modulates lipopolysaccharide (LPS) stimulation-induced normal human astrocyte proliferation and activation. Cytokine 131: 155106, 2020.
20. Zhang Q, Jin X, Shi W, Chen X, Pang W, Yu X and Yang L: A long non-coding RNA LINC00461-dependent mechanism underlying breast cancer invasion and migration via the miR-144-3p/KPNA2 axis. Cancer Cell Int 20: 137, 2020.
21. Cheng Q and Wang L: LncRNA XIST serves as a ceRNA to regulate the expression of ASF1A, BRWD1M, and PFKFB2 in kidney transplant acute kidney injury via sponging hsa-miR-212-3p and hsa-miR-122-5p. Cell Cycle 19: 290-299, 2020.
22. Tang Z, Li C, Kang B, Gao G, Li C and Zhang Z: GEPIA: A web server for cancer and normal gene expression profiling and interactive analyses. Nucleic Acids Res 45: W98-W102, 2017.
23. Fornes O, Castro-Mondragon JA, Khan A, van der Lee R, Zhang X, Richmond PA, Modi BP, Correard S, Gheorghe M, Baranašić D, *et al*: JASPAR 2020: update of the open-access database of transcription factor binding profiles. Nucleic Acids Res 48: D87-D92, 2020.
24. Netanely D, Stern N, Laufer I and Shamir R: PROMO: An interactive tool for analyzing clinically-labeled multi-omic cancer datasets. BMC Bioinformatics 20: 732, 2019.
25. Mas-Ponte D, Carlevaro-Fita J, Palumbo E, Hermoso Pulido T, Guigo R and Johnson R: LncATLAS database for subcellular localization of long noncoding RNAs. RNA 23: 1080-1087, 2017.
26. Cao Z, Pan X, Yang Y, Huang Y and Shen HB: The lncLocator: A subcellular localization predictor for long non-coding RNAs based on a stacked ensemble classifier. Bioinformatics 34: 2185-2194, 2018.
27. Li JH, Liu S, Zhou H, Qu LH and Yang JH: starBase v2.0: Decoding miRNA-ceRNA, miRNA-ncRNA and protein-RNA interaction networks from large-scale CLIP-Seq data. Nucleic Acids Res 42: D92-D97, 2014.
28. Chandrashekar DS, Bashel B, Balasubramanya SAH, Creighton CJ, Ponce-Rodriguez I, Chakravarthi BVSK and Varambally S: UALCAN: A portal for facilitating tumor subgroup gene expression and survival analyses. Neoplasia 19: 649-658, 2017.
29. Livak KJ and Schmittgen TD: Analysis of relative gene expression data using real-time quantitative PCR and the 2(-Delta Delta C(T)) method. Methods 25: 402-408, 2001.
30. Xu Z, Zhu C, Chen C, Zong Y, Feng H, Liu D, Feng W, Zhao J and Lu A: CCL19 suppresses angiogenesis through promoting miR-206 and inhibiting Met/ERK/Elk-1/HIF-1α/VEGF-A pathway in colorectal cancer. Cell Death Dis 9: 974, 2018.
31. Ma J, Liu X, Chen H, Abbas MK, Yang L, Sun H, Sun T, Wu B, Yang S and Zhou D: c-KIT-ERK1/2 signaling activated ELK1 and upregulated carcinoembryonic antigen expression to promote colorectal cancer progression. Cancer Sci 112: 655-667, 2021.
32. Yano S, Wu S, Sakao K and Hou DX: Involvement of ERK1/2-mediated ELK1/CHOP/DR5 pathway in 6-(methylsulfinyl)hexyl isothiocyanate-induced apoptosis of colorectal cancer cells. Biosci Biotechnol Biochem 83: 960-969, 2019.
33. Kent OA, Mendell JT and Rottapel R: Transcriptional regulation of miR-31 by oncogenic KRAS mediates metastatic phenotypes by repressing RASA1. Mol Cancer Res 14: 267-277, 2016.
34. Xu G, Zhang Y, Li N, Wu Y, Zhang J, Xu R and Ming H: LBX2-AS1 up-regulated by NFIC boosts cell proliferation, migration and invasion in gastric cancer through targeting miR-491-5p/ZNF703. Cancer Cell Int 20: 136, 2020.
35. Lu L, Cai M, Peng M, Wang F and Zhai X: miR-491-5p functions as a tumor suppressor by targeting IGF2 in colorectal cancer. Cancer Manag Res 11: 1805-1816, 2019.
36. Zhang J, Raju GS, Chang DW, Lin SH, Chen Z and Wu X: Global and targeted circulating microRNA profiling of colorectal adenoma and colorectal cancer. Cancer 124: 785-796, 2018.
37. Jung Y, Lee S, Choi HS, Kim SN, Lee E, Shin Y, Seo J, Kim B, Jung Y, Kim WK, *et al*: Clinical validation of colorectal cancer biomarkers identified from bioinformatics analysis of public expression data. Clin Cancer Res 17: 700-709, 2011.
38. Moravkova P, Kohoutova D, Vavrova J and Bures J: Serum S100A6, S100A8, S100A9 and S100A11 proteins in colorectal neoplasia: Results of a single centre prospective study. Scand J Clin Lab Invest 80: 173-178, 2020.
39. Wang G, Wang X, Wang S, Song H, Sun H, Yuan W, Cao B, Bai J and Fu S: Colorectal cancer progression correlates with upregulation of S100A11 expression in tumor tissues. Int J Colorectal Dis 23: 675-682, 2008.
40. Chang Y, Li N, Yuan W, Wang G and Wen J: LINC00997, a novel long noncoding RNA, contributes to metastasis via regulation of S100A11 in kidney renal clear cell carcinoma. Int J Biochem Cell Biol 116: 105590, 2019.
41. Niu Y, Shao Z, Wang H, Yang J, Zhang F, Luo Y, Xu L, Ding Y and Zhao L: LASP1-S100A11 axis promotes colorectal cancer aggressiveness by modulating TGFβ/Smad signaling. Sci Rep 6: 26112, 2016.